3.7 The general shape of fields, charges, and currents on a transmission line 1
(a) E_θ at a conductor surface vanishes 1
(b) The scalar potential φ on a conductor surface 2
(c) B and A_z on a conductor surface 5
(d) Observations about the E and B field lines in a transmission line dielectric 7
(e) Drawings of the fields 9
(f) More on the field and current structure 11
(g) Estimate of the ratio J_r/J_z 13
3.8 Transmission Line Preliminaries 15

3.7 The general shape of fields, charges, and currents on a transmission line

(a) E_θ at a conductor surface vanishes

We start by borrowing Fig B.6 from Appendix B,

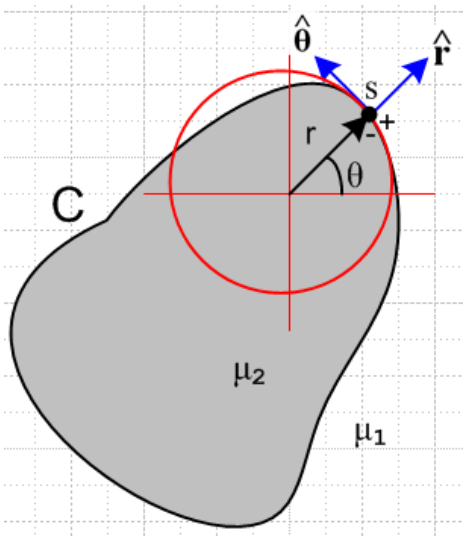

Fig B.6

The figure shows a transmission line conductor of some arbitrary (but reasonably smooth) cross section shape. At the point of interest **s** we construct a cylindrical coordinate system as shown, such that the coordinates (r,θ,z) are appropriate for point **s** and its immediate neighborhood. Basically we approximate the piece of conductor surface near **s** as if it were the surface of a round wire of some radius r. At this point **s**, then, we can talk about fields E_θ, E_r, B_θ, and B_r.

For a transmission line we shall use $\mathbf{E_t}$ to refer to the transverse components of an electric field, as opposed to the longitudinal component E_z. In Cartesian coordinates $\mathbf{E_t} = (E_x,E_y)$ and in the local cylindrical coordinates just defined at a surface point **s**, $\mathbf{E_t} = (E_r,E_\theta)$. The important point is that E_θ is our notation for the component of $\mathbf{E_t}$ which at some surface point is tangent to the surface, while E_r is normal to the surface.

A fundamental assumption of transmission line theory is that the cross-section tangential electric field at a conductor surface vanishes, which is to say, E_θ as defined above vanishes at all points on the surface. This assumption is examined in Appendix D.8 and here we accept it as fact. The basic idea is that surface charge is free to move along the conductor surface in a z=constant plant to neutralize any E_θ that might develop, and this mechanism of maintaining $E_\theta = 0$ on the surface works from DC up to perhaps 1000 GHz.

Fact 1: $E_\theta = 0$ at the surface of a transmission line conductor. (3.7.1)

This assumption, stated in partial waves, appears in (D.2.27) and is one of two boundary conditions used in that Appendix to determine the internal fields of a round wire, the other boundary condition being (D.2.26). One can consider Fact 1 to be part of the "quasi-static" model of a transmission line.

(b) The scalar potential φ on a conductor surface

By "conductor surface" we mean the boundary of a cross-sectional slice at z = constant through a transmission line conductor. In electrostatics one has $\mathbf{E} = -\nabla\varphi$ and then $\mathbf{E}_t = \nabla_t\varphi$ for the transverse electric field. In the neighborhood of a surface point **s** we write this as $E_\theta = (1/r)\partial_\theta\varphi$ and $E_r = \partial_r\varphi$. Since Fact 1 says $E_\theta = 0$ at any **s** on the surface, we conclude that φ = constant all the way around the conductor boundary. This is fine for ω = 0, but for ω > 0 we have from (1.3.1) that $\mathbf{E} = -\nabla\varphi - j\omega\mathbf{A}$ and so

$$\mathbf{E}_t = -\nabla_t\varphi - j\omega\mathbf{A}_t \tag{3.7.2}$$

and now it is no longer possible to immediately claim $E_\theta = 0 \Rightarrow \varphi$ = constant on the boundary. We shall now show that, under suitable conditions, the last term $-j\omega\mathbf{A}_t$ is much smaller (in magnitude) than the first term $-\nabla_t\varphi$, and therefore we have $\mathbf{E}_t \approx -\nabla_t\varphi$ and then φ ≈ constant by our argument above.

An arm-waving argument is to say that the transverse potential $\mathbf{A}_t$ can be neglected in a transmission line and therefore $\mathbf{E}_t \approx -\nabla_t\varphi$, but we shall try to do better with a more substantial argument.

First, we shall divide up the frequency domain (relative to some transmission line geometry) into a set of regimes. We state these for a round wire of radius a, but for a general conductor one can replace a with some typical transverse dimension of the conductor :

$\delta > a/10$	$\delta < a/10$	$\delta < a/1000$	
low frequency	strong skin effect	extreme skin effect	(3.7.3)

Here $\delta \equiv \sqrt{2/(\omega\mu\sigma)}$ is the skin depth of (2.1.8) or (2.2.20). Obviously the classification is arbitrary. We shall find that some facts which are approximately valid for the strong skin effect regime are almost exactly valid in the extreme skin effect regime.

Here then is what we want to show:

Fact 2: $\varphi \approx$ constant on a conductor surface in the strong or extreme skin effect regimes within the Transmission Line Limit. (3.7.4)

Our proof proceeds in a set of steps (the Transmission Line Limit is defined in Step 4).

Step 1. In the strong or extreme skin depth regime, $A_z \approx (1/v_d)\,\varphi$. (3.7.5)

The subscript "d" refers to a value in the dielectric between conductors, and here $v_d = 1/\sqrt{\mu_d \varepsilon_d}$ is the speed of light in the dielectric and also the phase velocity of a wave going down our transmission line. Similarly, $\beta_d = (\omega/v_d)$ is the wave's wavenumber in the dielectric. Using $\partial_z \rightarrow -j\beta_d$ as in (D.1.16) and our usual $\partial_t \rightarrow j\omega$ we find from (1.3.1) that

$$E_z = j\beta_d\varphi - j\omega A_z = j(\omega/v_d)\varphi - j\omega A_z = j\omega\,[\,\varphi/v_d - A_z\,]\,. \qquad \beta_d = (\omega/v_d) \tag{3.7.6}$$

In the strong or extreme skin depth regime, ω is large and the left side of (3.7.6) is much smaller than the right side. We can write $\varphi/v_d - A_z = E_z/(j\omega)$. In the limit $\delta \rightarrow 0$ we would have $E_z = 0$, but such a limit is not reached in a practical transmission line, so for small δ we can only conclude that E_z/ω is very small. Therefore,

$$A_z \approx \varphi/v_d \qquad \text{small or extreme skin effect} \tag{3.7.7}$$

Sometimes a different argument is given to obtain (3.7.7). In the King gauge we know from (1.5.5) that in the dielectric,

$$\text{div}\,\mathbf{A} = -j\,(\beta_d^2/\omega)\varphi \tag{1.5.5}$$

or

$$(\partial_x A_x + \partial_y A_y) + \partial_z A_z = -j\,(\beta_d^2/\omega)\varphi$$

or

$$(\partial_x A_x + \partial_y A_y) - j\beta_d A_z = -j\,(\beta_d^2/\omega)\varphi\ . \tag{3.7.8}$$

Without a proof, we extend that usual arm-waving argument that $\mathbf{A}_t$ components can be neglected to say that transverse *derivatives* of $\mathbf{A}_t$ can also be neglected so $(\partial_x A_x + \partial_y A_y) \approx 0$, and then we have

$$-j\beta_d A_z \approx -j\,(\beta_d^2/\omega)\varphi$$

or

$$A_z \approx (\beta_d/\omega)\varphi = \varphi/v_d$$

which replicates the conclusion (3.7.7) seemingly without the skin effect restriction. A more careful analysis must show that $(\partial_x A_x + \partial_y A_y)$ can only be so neglected in the strong or extreme skin effect limits.

Step 2. Claims that $|\nabla_t\varphi| \approx (1/D)|\varphi|$ where D is a characteristic transverse dimension of the transmission line.

We might argue this on dimensional grounds alone, but consider

$$|\partial_x \varphi| \approx \frac{\Delta\varphi}{\Delta x} \approx \frac{V}{D} \approx (1/D)\,|\varphi| \ . \qquad (3.7.9)$$

This is a very crude use of the ≈ sign, there could be a factor of 10 or 1/10 on either side, but when combined with << in Step 4 below we still obtain a reasonable conclusion. Here V is the potential difference between the two transmission line conductors, and D is their "separation". Obviously $|\partial_x \varphi|$ is not the exact constant V/D at every point in space between the conductors, this is meant only as a ballpark estimate of the size of $|\partial_x \varphi|$ in some average sense.

Step 3. Claims that $|\omega A_x| << 2\pi\,|\varphi|\,(1/\lambda)$ where λ = wave's wavelength.

Appendix M shows that for a transmission line $|\mathbf{A}_t| < 10^{-4}\,|A_z|$ for f = DC to 1000 GHz, and this is then a quantitative statement of the fact that "the transverse vector potential is small". The basic idea is that in a transmission line the major current is in the z direction, and $\mathbf{A} \sim \mathbf{J}$ according to the Helmholtz integral. Then since $|J_t| << |J_z|$, one finds that $|A_t| << |A_z|$.

So we start then with (using the x transverse component of A_t)

$$|A_x| << |A_z| \,. \qquad (3.7.10)$$

With (3.7.7) this says

$$|A_x| << |\varphi| / v_d = |\varphi|\ (\beta_d/\omega)$$

or

$$|\omega A_x| << (2\pi/\lambda)\,|\varphi| \qquad \beta_d = 2\pi/\lambda \qquad (3.7.11)$$

where λ is the wavelength of our transmission line wave.

Step 4. Claims that $|\omega A_x| << |\partial_x \varphi|$

In Chapter 4 we shall introduce the notion of the Transmission Line Limit which is a requirement that on a transmission line, the wavelength λ must be much larger than any transverse dimension D of the line,

$$\lambda >> D \qquad (3.7.12)$$

or

$$(1/\lambda) << (1/D)$$

or

$$2\pi\,|\varphi|\,(1/\lambda) << 2\pi\,|\varphi|\,(1/D) \qquad (3.7.13)$$

Combining this with (3.7.11) we find

$$|\omega A_x| << (2\pi/\lambda)\,|\varphi| << 2\pi\,|\varphi|\,(1/D)$$

or

$$|\omega A_x| << 2\pi\,|\varphi|\,(1/D) \,.$$

Bringing in the ballpark estimate (3.7.9) that $|\partial_{\mathbf{x}}\varphi| \approx (1/D)\,|\varphi|$ we then have

$$|\omega A_{\mathbf{x}}| << |\partial_{\mathbf{x}}\varphi|$$

where we just ignore the 2π factor relative to our extreme << situation. Doing this also for y, we have

$$|\omega \mathbf{A}_{\mathbf{t}}| << |\nabla_{\mathbf{t}}\varphi| \tag{3.7.14}$$

Looking then at (3.7.2) one finds

$$\mathbf{E}_{\mathbf{t}} = -\nabla_{\mathbf{t}}\varphi - j\omega\mathbf{A}_{\mathbf{t}} \approx -\nabla_{\mathbf{t}}\varphi \tag{3.7.15}$$

and this concludes our longwinded explanation of why $\varphi \approx$ constant on a transmission line conductor's cross section surface. We had to assume the Transmission Line Limit ($\lambda >> D$) and we had to assume the strong or extreme skin effect regime to get $\varphi \approx$ constant

The fact that $\varphi \approx$ constant on each conductor surface is then an extension of the quasi-static transmission line theory. We know that φ = constant at $\omega = 0$, but in order to prove that φ = constant at $\omega > 0$ we have to make the extra assumptions stated in the last paragraph. We have not provided any proof that φ = constant for the "low frequency" range of (3.7.3), except for $\omega = 0$. In Chapter 4, we shall have to assume the strong or extreme skin effect regime anyway in order to arrive at the classical transmission line equations, so we won't worry about this low frequency range of ω.

(c) B and A_z on a conductor surface

From Appendix M we know that $|A_{\mathbf{x},\mathbf{y}}| << A_{\mathbf{z}}$ for a transmission line, and so we just set $A_{\mathbf{x}} = A_{\mathbf{y}} \approx 0$. In this case we find that

$$\mathbf{B} = \text{curl}\,\mathbf{A} = \hat{\mathbf{x}}\,(\partial_{\mathbf{y}}A_{\mathbf{z}} - \partial_{\mathbf{z}}A_{\mathbf{y}}) + \hat{\mathbf{y}}\,(\partial_{\mathbf{z}}A_{\mathbf{x}} - \partial_{\mathbf{x}}A_{\mathbf{z}}) + \hat{\mathbf{z}}\,(\partial_{\mathbf{x}}A_{\mathbf{y}} - \partial_{\mathbf{y}}A_{\mathbf{x}})$$

$$= \hat{\mathbf{x}}\,(\partial_{\mathbf{y}}A_{\mathbf{z}}) + \hat{\mathbf{y}}\,(-\partial_{\mathbf{x}}A_{\mathbf{z}}) = \mathbf{B}_{\mathbf{t}} \tag{3.7.16}$$

which says $\mathbf{B} \approx \mathbf{B}_{\mathbf{t}}$ is mainly in the transverse direction. In the extreme skin effect, we know that inside the conductor **B** decays to 0 quickly over distance δ (see Fig 2.9 for an isolated round wire). This is akin to the Meissner Effect where magnetic fields are excluded from the interior of a superconductor. Just below the thin current sheath we then have $B_{\mathbf{r}} = 0$, where $B_{\mathbf{r}}$ is the component of $\mathbf{B}_{\mathbf{t}}$ normal to the surface. According to box (1.1.50) we know that $B_{\mathbf{r}}$ is continuous through the boundary, so we must have $B_{\mathbf{r}} = 0$ just *outside* the surface as well. Thus we conclude that :

Fact 3: In the extreme skin effect regime, the **B** field at a transmission line conductor surface has a negligible z component and is mainly tangential to the conductor, having a negligible normal component. This is approximately true in the strong skin effect regime. (3.7.17)

Corollary: In the plane of a transmission line conductor cross section, and in the extreme skin effect regime, the magnetic field line pattern in the dielectric is such that just above the surface of each

conductor there is a closed tangential B field line enclosing the conductor which is almost exactly parallel to the surface at every point. This fact is approximately true for the strong skin depth regime. (3.7.18)

This is illustrated in the following figure where B field lines are shown in red:

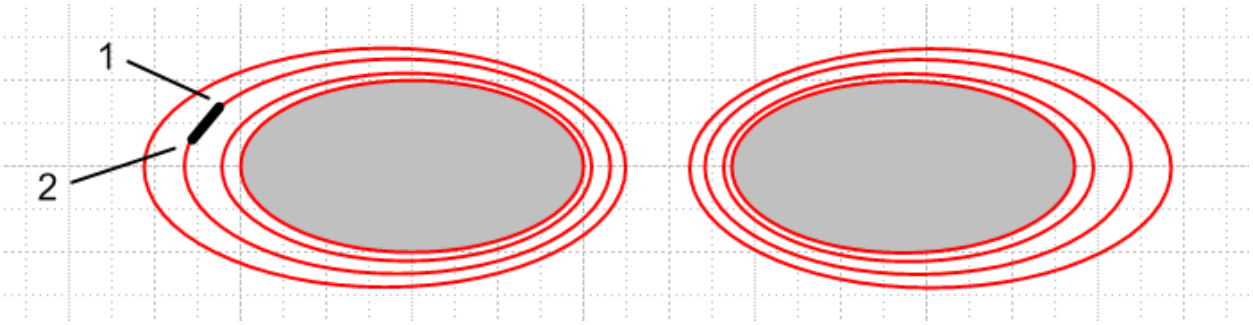

Fig 3.5

Fact 4: In a situation where $A_{x,y}$ can be neglected relative to A_z we have seen that the B field lines are constrained to cross sectional planes. For any such planar set of B field lines, each B field line is an equipotential contour for A_z. (3.7.19)

Proof: Consider a small rectangular "math loop" into the plane of paper (depth dz) as shown in the above Figure. The black segment shows this loop edge on. Since this loop is parallel to the B field lines, the magnetic flux through the loop is zero. According to (1.1.39) we know that

$$\text{curl } \mathbf{A} = \mathbf{B} \quad \Leftrightarrow \quad \oint_C \mathbf{A} \bullet d\mathbf{s} = \int_S \mathbf{B} \bullet d\mathbf{S} \,. \qquad (1.1.39)$$

The line integral of **A** around our math loop must therefore vanish. But since **A** has only the component A_z, the line integral has contributions only from the two sides of the loop (both of which are perpendicular to paper). Thus $\oint_C \mathbf{A} \bullet d\mathbf{s} = [\, A_z(1) - A_z(2) \,]\, dz = 0$ so $A_z(1) = A_z(2)$. By this argument, all points on the red B field line shown have the same value of A_z and thus that red B field line is an equipotential contour for A_z. But this applies to any of the red B field lines, so in general, each such B field line is an equipotential for A_z.

Fact 5: On each conductor boundary, $A_z \approx$ constant in the extreme or strong skin effect regimes. (3.7.20)

From (3.7.18) we know that in the extreme skin depth regime, the innermost B field line almost exactly skirts the conductor perimeter. From (3.7.19) we know that any B field line is an equipotential contour. Thus, the cross section perimeter itself is very close to an equipotential contour of the function $A_z(x,y,z)$. In the strong skin effect regime this constancy of A_z on the boundary is only approximately true.

Comment: In Fact 2 we argued that $\varphi \approx$ constant on a conductor perimeter in the extreme skin effect regime. We also argued that $A_z \approx (1/v_d)\varphi$ everywhere inside the conductor and therefore also at the conductor surface. Thus, Fact 2 that $\varphi \approx$ constant on the perimeter is consistent with Fact 5 that $A_z \approx$ constant on the perimeter, and in fact these two constants are related by $A_z \approx (1/v_d)\, \varphi$. That is,

A_z(any point on perimeter) $\approx (1/v_d)\,\varphi$(any point on perimeter) //extreme δ (3.7.21)

and for the strong δ regime, this is approximately true.

A Counter Example. We have argued above that in the strong skin effect limit, the perimeter of a transmission line conductor's cross section will align with a B field line and will have a constant value of A_z. This is in general NOT true for low frequencies. In particular, it is not true at $\omega = 0$. As an example of this fact, we consider a pair of parallel round wires carrying current I and -I . Since the current density in the wires is uniform, it is an easy matter to compute **B** for each conductor and superpose to get the total **B** field due to both conductors. We can also do this for the vector potential component A_z , as detailed in Appendix G. Here is a plot of the resulting magnetic field lines:

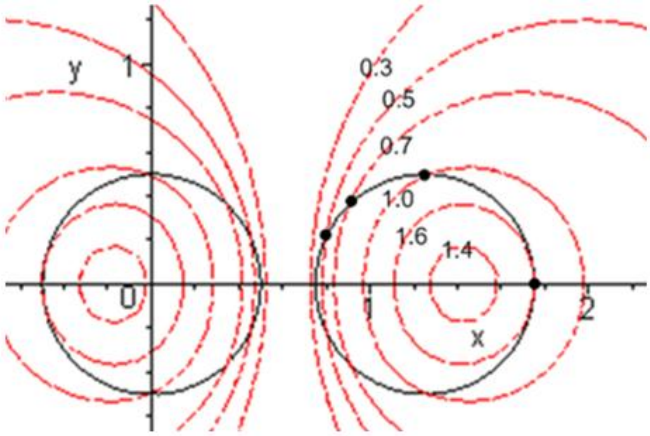

Fig 3.6

The conductor perimeters are shown as black circles, and it is clear that these circles do not coincide with any magnetic field contours (shown in red). The numbers indicate the relative value of A_z on the different red B field contours, and once sees that A_z is not a constant on the black conductor surfaces.

Having said this, we might still claim in a very *ballpark* sense that the black circles very crudely align with the magnetic field lines (with perhaps a 30% spatial mismatch), and that the conductor black circles are crudely equipotentials for A_z, since A_z only varies between 0.4 and 1.6 in this example, and not say between .001 and 1000. But this is really too crude to support the transmission line theory presented later, and so that theory will be restricted to the strong and extreme skin effect regimes.

(d) Observations about the E and B field lines in a transmission line dielectric

Fact 6: In a *cross sectional* sketch of a transmission line, the **E** field lines land on the conductors at right angles to the conductor surface. This is exactly true for the TEM mode, and applies to all points on the conductor surfaces. (3.7.22)

Proof: This follows from Fact 1 (3.7.1) which says $E_\theta = 0$ at the conductor surface.

Fact 7: In a *longitudinal* sketch of a transmission line, the E field lines still land on the conductors at very close to right angles. (3.7.23)

Proof: Although $E_\theta = 0$ at the conductor surface, E_z is not zero, though it is very small. We know that E_z exists inside the conductor to support $J_z = \sigma E_z$, and we know by (1.1.41) that E_z is continuous through the boundary, so the longitudinal landing angle will not quite be $\pi/2$. The deviation from $\pi/2$ is less than 10^{-4} radians according to (3.6.2), and the deviation is in the direction of current flow at each conductor. This causes a very slightly warping of the otherwise planar cross-sectional field line grid.

Fact 8: Apart from an overall scale factor, the cross-sectional field shape of a TEM wave on a transmission line is independent of position z along the transmission line, and is independent of time t. The shape is also independent of ω. (3.7.24)

Proof: As we shall see below, the TEM form of any field or current is $\mathbf{F}(x,y,z,t) = e^{j[\omega t - kz + \varphi_F(\omega)]}\mathbf{F}(x,y)$ where $\mathbf{F}(x,y)$ is real and all t and z dependence is in the exponential. We can take the physical field to be the real part as discussed in Section 1.6 so $\mathbf{F}_{physical}(x,y,z,t) = \cos[\omega t - kz + \varphi_F(\omega)]\ \mathbf{F}(x,y)$. Thus, the cross sectional shape of the field is determined by $\mathbf{F}(x,y)$ and is the same at all values of z apart from an overall scale factor $\cos[\omega t - kz + \varphi_F(\omega)]$. This scale factor varies between +1 and -1 as one moves down the line in z at some fixed t, or as one observes at some fixed z as time varies. Later we will see that this shape $\mathbf{F}(x,y)$ can be found by solving a certain 2D Helmholtz equation, and we find that the shape is determined entirely by the shape of the boundaries of the conductors. Different vector fields (e.g., **J** and **E**) might have different ω-dependent phases in this wave motion which we indicate by $\varphi_F(\omega)$ for $\mathbf{F}(x,y,z,t)$.

Fact 9: In a cross sectional sketch of a transmission line operating in the extreme skin effect regime, the **E** and **B** field lines are very nearly perpendicular at every point in the dielectric. In the strong skin effect regime, the fields are approximately perpendicular. (3.7.25)

Proof: From Maxwell's curl E equation (1.1.2) in the ω domain we have

$$\text{curl } \mathbf{E} = -j\omega\mathbf{B} \ . \qquad (1.1.2)$$

Then

$$\mathbf{B} \bullet \mathbf{E} = (-j\omega)^{-1}\ \mathbf{curl\ E} \bullet \mathbf{E}$$

$$= (-j\omega)^{-1} \left[\left(\partial_x E_y - \partial_y E_x \right) E_z + \left(\partial_y E_z - \partial_z E_y \right) E_x + \left(\partial_z E_x - \partial_x E_z \right) E_y \right] . \qquad (3.7.26)$$

In the extreme skin effect regime, for a given ω we think of conductivity σ being very large, and so the conductor's E_z is very small. Since E_z is continuous at the conductor boundary, E_z is also very small in the dielectric. In contrast, due to the surface charge on the conductors, the transverse fields E_x and E_y are very large in the dielectric. If we neglect E_z and its derivatives in the above expression we find that

$$\mathbf{B} \bullet \mathbf{E} \approx (-j\omega)^{-1} \left[\left(-\partial_z E_y \right) E_x + \left(\partial_z E_x \right) E_y \right]$$

$$\approx (-j\omega)^{-1} \left[E_y^2\, \partial_z (E_x / E_y) \right] . \qquad (3.7.27)$$

However, we argued in Fact 8 that the shape of fields does not vary with z. Thus, the ratio of two components like E_x/E_y cannot vary with z, so $\partial_z(E_x/E_y) = 0$. Alternatively, we make the usual replacement $\partial_z \rightarrow -j\beta_d$ to get

$$\mathbf{B} \bullet \mathbf{E} \approx (-j\omega)^{-1} [(-\partial_z E_y)E_x + (\partial_z E_x)E_y] = (-j\omega)^{-1} [(j\beta_d E_y)E_x + (-j\beta_d E_x)E_y]$$

$$= (-j\omega)^{-1})(j\beta_d) [(E_y)E_x + (-E_x)E_y]$$

$$= 0 \ . \qquad (3.7.28)$$

We have already shown that at the conductor surfaces, **E** is normal to the surface and in the extreme skin effect regime **B** is nearly tangent to the surface, so we certainly have $\mathbf{B} \bullet \mathbf{E} \approx 0$ at the conductor surfaces.

(e) Drawings of the fields

We are now in a position to draw some sketches of fields on a transmission line. Let's start with the transverse or cross section picture:

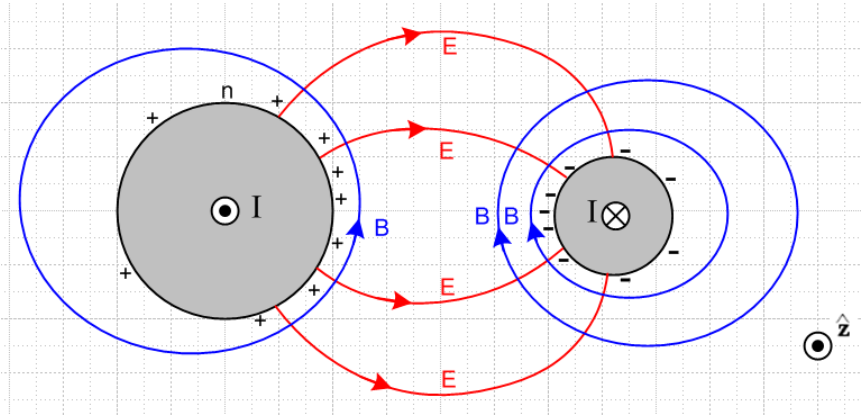

Fig 3.7: Cross section view

Fig 3.7

Although this figure is drawn for two round conductors, its general features apply to any conductors. The figure is a snapshot at one instant in time. The • and ⊗ indicate current flow direction in the conductors. Positive charge exists on the surface of the left conductor, and is strongest on the face of that conductor which is closest to the other conductor. Negative surface charge lies on the right conductor. The electric fields are as shown and are strongest in the region between the conductors. The magnetic field directions derive from the right hand rule relative to the current in each conductor. The lines of E and B always intersect at right angles as noted in (3.7.25).

The magnitude of the E field is determined by the potential difference between the conductors and the geometry. It is independent of frequency. Similarly, the magnitude of the B field is determined by the size of the current in either conductor and is also independent of frequency.

Consider a 75 Ω transmission line that is properly terminated and is driven by a 7.5 volt amplitude sine wave. Regardless of frequency ω, the magnitude of the current in this transmission line is 100 mA, and the magnitude of the potential difference is 7.5 volts. Of course both these quantities have sinusoidal time dependence. At some instant in time, the fields and currents are as in Fig 3.7.

We have just argued then that not much happens in the transverse directions x and y as frequency sweeps up from strong skin effect to extreme skin effect. Of course the rate at which the pattern oscillates back and forth increases, but the shape of things does not change. At the peak of each cycle, things look like Fig 3.7 regardless of ω.

This may seem contradictory. In general, one is used to ω affecting things due to equations like

curl **E** = -jω**B** Maxwell curl E equation *(1.1.2)*

The resolution is that all the spatial variation happens in the *longitudinal* direction. Here then is a top view of the same transmission line:

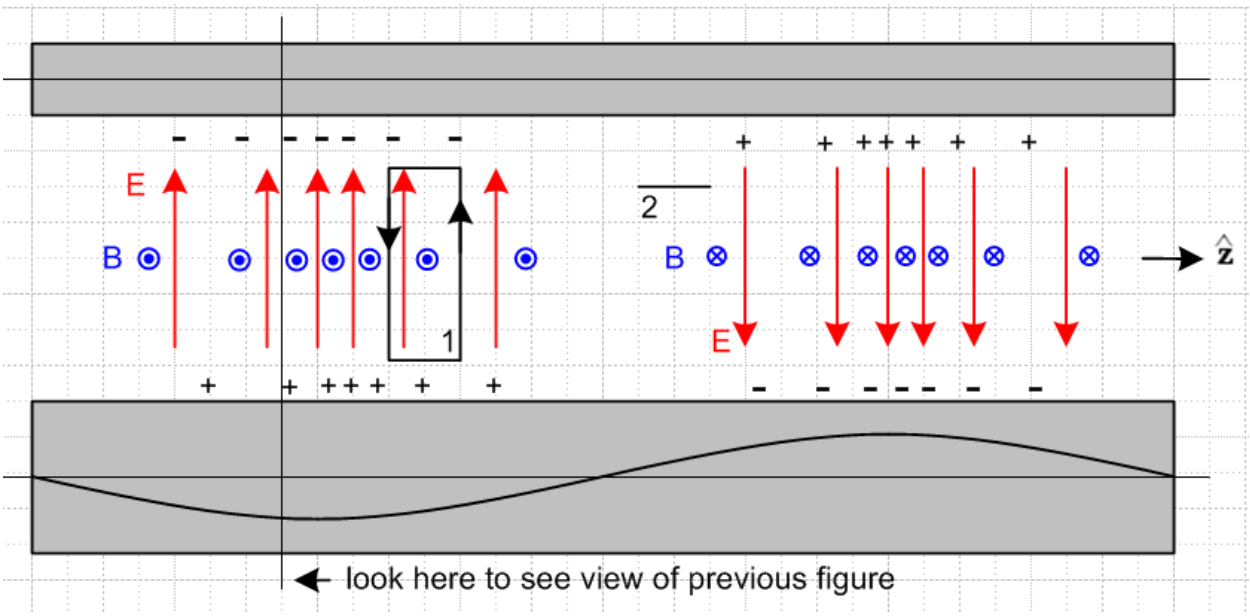

Fig 3.8: Top view of transmission line Fig 3.8

The red E arrows are all of unit length and serve to mark the direction and density of electric field lines lying in the plane containing the center lines of the conductors. The blue B arrows are seen end-on and indicate the same for the magnetic field. On the left they come out of the plane of paper and on the right they go into it. Later we shall learn about the "transmission line limit" in which the wavelength λ of the wave propagating down a transmission line is assumed to be much larger than all transverse dimensions of the line. The reader should understand the above picture as being in that limit, but one would have to stretch the picture at least 10X horizontally to make it be reasonable. At all places **E**x**B** points to the right, so we have a wave propagating to the right (+z).

Now apply the Maxwell curl equations using the two loops shown. Loop 1 is positioned to pick up magnetic flux, so we use (1.1.36) which in the frequency domain says

curl **E** = -jω**B** $\Leftrightarrow$ $\oint \mathbf{E} \bullet d\mathbf{s} = -j\omega[\int_S \mathbf{B} \bullet d\mathbf{S}]$ (3.7.29)

Notice the ω sitting on the right side. We argued in the last section that the amplitude of the B field does not change as ω changes. Thus, the right side of (3.7.29) is proportional to ω. As ω increases, the line integral of the E field around loop 1 must increase. Thus, the rate of change of E must increase in the z direction! In other words, as ω increases, the whole pattern of Fig 2 contracts in the z direction, which causes all z derivatives to increase, thus increasing $\oint \mathbf{E} \cdot \mathbf{ds}$ for the same fixed loop 1. Remember that the strength of the E field is indicated in Fig 2 by the density of the red arrows, not by the length of the red arrows.

A similar argument applies to loop 2. This loop appears end-on in Fig 3.8. It is set up to sense the electric field flux. The appropriate curl equation is (1.1.38) which says

$$\text{curl } \mathbf{B} = \mu\varepsilon j\omega \mathbf{E} + \mu \mathbf{J_c} \qquad \Leftrightarrow \qquad \oint \mathbf{B} \bullet d\mathbf{s} = \mu \int_S [\varepsilon j\omega \mathbf{E} + \mathbf{J_c}] \bullet d\mathbf{A}$$

$$\approx j\omega\mu\varepsilon \int \mathbf{E} \cdot d\mathbf{A} \, . \qquad (3.7.30)$$

Since we are now in the dielectric, we have ignored the small leakage conduction current, and have kept the dominant displacement current. Again there is a factor of ω on the right side, arising from a time derivative. As ω increases, the line integral of the B field must increase. Thus, the B field must change faster in the z direction. As ω increases, the curl equation (3.7.30) is satisfied by having the entire pattern contract in the z dimension.

If the frequency ω doubles, the wavelength λ goes to half. This of course is no surprise, since ω and λ are related by the speed of light v_d in the dielectric,

$$\lambda = v_d/f = 2\pi v_d/\omega \, . \qquad (3.7.31)$$

The main point of the above discussion is to show how the Maxwell curl equations force the field pattern to contract in the z direction as ω increases. In the transverse direction, the field pattern *shape* stays constant.

(f) More on the field and current structure

Here we explore in more detail the general distribution of fields and currents in a transmission line. The goal is to establish the phase relationships among the electromagnetic fields and various currents. Once this is done, it is possible to make an estimate of the ratio J_r/J_z and that is done in the following section.

Consider the following more elaborate version of Figure 3.8 :

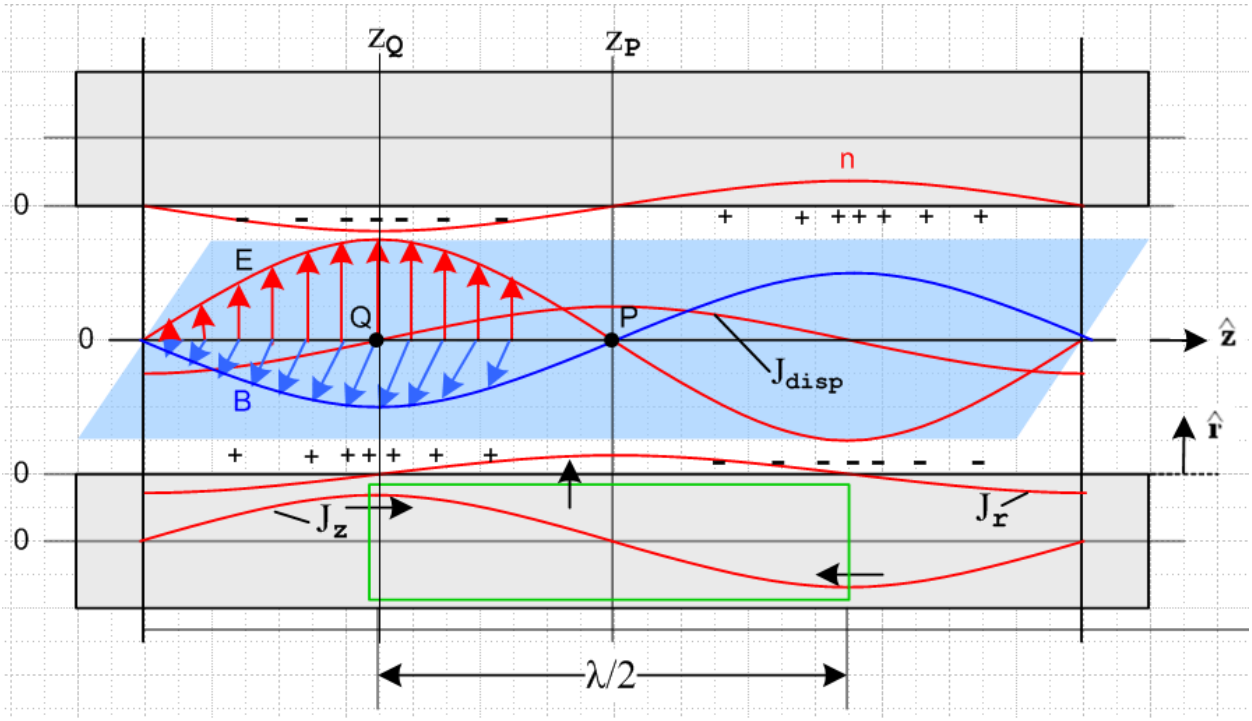

Tilted overhead view of a transmission line Fig 3.9

The picture is quite complicated and deserves clarifying comments:

(1) Unlike in Fig 3.8, the E and B arrows indicate the **E** and **B** vectors, and are not just field direction and field line density indicators.

(2) The **E** and **B** field vectors are shown along some line which lies in the plane of the center lines of the two conductors and which points in the $\hat{\mathbf{z}}$ direction, as do those center lines.

(3) The blue **B** field arrows lie in the blue plane which is meant to be perpendicular to the plane of the conductor center lines, which is the plane of paper. The red **E** field arrows are in the plane of paper.

(4) Looking at **E** x **B**, we see that the wave is traveling to the right in the $\hat{\mathbf{z}}$ direction.

(5) The **E** field arrows point from positive charge to negative charge, so this is why the + and - signs are distributed as shown.

(6) The conductors are fixed to the paper, everything else is moving to the right at velocity v_d. This includes the **E** and **B** arrows and their curves, the charge density and its curve n, and the two current curves drawn on the bottom conductor.

(7) At point Q on plane $z = z_Q$, since **B** is coming out of paper to the viewer, the longitudinal current J_z in the lower conductor must be pointing to the right. This is why J_z is shown positive at this point in the lower conductor, and this calibrates the position of the J_z curve. Maximum J_z occurs with maximum B.

(8) There exists a displacement current $\mathbf{J_{disp}} = \partial_t \mathbf{D} = \varepsilon\, \partial_t \mathbf{E}$ in the dielectric whose magnitude is shown as a red curve. For an observer sitting at fixed point P, since the wave is moving to the right, the value of $\partial_t \mathbf{E}$ is at its instantaneous maximum positive value. This is why the red J_{disp} curve has a positive maximum at point P.

(9) As discussed in Section 3.4, the displacement current is "fed" by the radial current J_r inside the lower conductor, so the J_r curve also has its maximum positive value at point P. This J_r current is busily radially pumping positive charge to the surface of the lower conductor at point P so that charge will be there when the wave has moved $\lambda/4$ to the right. Of course this radial J_r is doing this charge pumping all around the lower conductor, but we only show it in the plane of paper.

(10) We have glossed over the fact that the E and B fields track each other in magnitude. For example, they are both maximal at the same longitudinal position z_Q. B is maximum there because J_z is maximum, but it is not quite clear why E is maximal at the same point. We know this alignment occurs in a plane wave, but a transmission line TEM mode is not *just* a plane wave. Various arguments can be ginned up for the alignment of the E and B maximums. One simple argument involves the green cylindrical Gaussian box drawn inside the lower conductor, and we reverse the discussion above. Note that this box lies entirely inside the conductor and so does not enclose any surface charge. Since there can be no charge inside a conductor, this box has $Q_{enclosed} = 0$. Thus, the total current flowing into this box must be zero. Since the J_z current flows into both ends of this box (black arrows), the J_r current has to flow out on the cylinder's curved surface. By considering shorter green boxes one can show that J_r is maximal at z_P (as drawn). Thus J_{disp} is maximum at z_P which means $\partial_t E$ must be maximum there, which means E = 0 at z_P which means E has its maximum in alignment with the maximum of B.

(g) Estimate of the ratio J_r/J_z

Having drawn and described this elaborate picture, we now consider again the green Gaussian box. At the instant in time for which Fig 3.9 is drawn, the total current flowing into the endcaps of the box is 2I, where I is the peak longitudinal current -- the magnitude of the longitudinal sine wave. Therefore, the total J_r integrated over the sides of the green cylinder must also be 2I.

To obtain a ballpark estimate of the situation, we first assume that the two round conductors are far apart compared to their radii, in which case J_r is roughly symmetric around the conductor surface. Then the total radial current emitted by the curved surface of the green Gaussian cylinder is:

$$\text{radial current total} = [\,(2/\pi)J_r\,]^* 2\pi a * (\lambda/2) = 2I$$

Since J_r is a longitudinal sine wave, we have added a factor $2/\pi$ to get its value averaged over the length of the Gaussian box. In a more general case, we can replace $2\pi a$ with distance p which represents the active portion of the conductor perimeter, as illustrated in Fig 2.14. Then we have

$$[\,(2/\pi)J_r\,]^* p * (\lambda/2) = 2I \quad \Rightarrow$$

$$J_r = 2\pi I / (\lambda p) \quad . \tag{3.7.32}$$

On the other hand, for a round conductor operating in the strong skin effect regime

$$J_z \approx I/(p\delta) \tag{3.7.33}$$

where p is the same active perimeter just mentioned. So

$$J_r/J_z \approx 2\pi\,(\delta/\lambda)\ . \qquad (3.7.34)$$

For δ we had

$$\delta \equiv \sqrt{2/\omega\mu\sigma}\ . \qquad \textit{(2.2.20)}$$

From (3.7.31) we have $\lambda = v/f = 2\pi v/\omega$ where v is the wave phase velocity. Then

$$(\delta/\lambda) = \sqrt{\frac{2}{\omega\mu\sigma}}\ \frac{\omega}{2\pi v} = \sqrt{\frac{2\omega}{\mu\sigma}}\ \frac{1}{2\pi v} = \sqrt{\frac{4\pi f}{\mu\sigma}}\ \frac{1}{2\pi v}\ . \qquad (3.7.35)$$

Setting $v \approx c$ and $\mu = \mu_0 = 4\pi \times 10^{-7}$ and $\sigma = 5.81 \times 10^{7}$ (copper) and $f = 10^{9} f(\text{Ghz})$ we get

$$(\delta/\lambda) \approx \sqrt{\frac{4\pi f}{\mu\sigma}}\ \frac{1}{2\pi v} = \sqrt{\frac{4\pi\ 10^{9}\ f(\text{GHz})}{4\pi \times 10^{-7} \times 5.81 \times 10^{7}}}\ \frac{1}{2\pi}\ \frac{1}{3 \times 10^{8}}$$

$$= \sqrt{\frac{10^{10}\ f(\text{GHz})}{58.1}}\ \frac{1}{2\pi}\ \frac{1}{3 \times 10^{8}} = \sqrt{\frac{f(\text{GHz})}{58.1}}\ \frac{1}{6\pi}\ 10^{-3} = 7 \times 10^{-6}\ \sqrt{f(\text{GHz})}$$

and so

$$J_r/J_z \approx (2\pi)\,(\delta/\lambda) \approx 4.4 \times 10^{-5}\ \sqrt{f(\text{GHz})}\ . \qquad (3.7.36)$$

For $f \leq 10$ GHz we then find

$$J_r/J_z \leq 1.4 \times 10^{-4}\ . \qquad f \leq 10\ \text{GHz} \qquad \text{strong skin effect regime} \qquad (3.7.37)$$

showing that the radial charge-pumping current density J_r is much smaller than the longitudinal current density J_z in the conductor sheath.

What about the low-frequency situation with no skin-effect sheath? For simplicity, we assume now two round conductors of radius a which are widely spaced. No skin effect means roughly $\delta > a$ which means

$$\sqrt{2/\omega\mu\sigma} > a \qquad \Rightarrow \qquad \omega < 2/(\mu\sigma a^2) \qquad \text{or} \qquad \omega a/2 < 1/(\mu\sigma a)\ . \qquad (3.7.38)$$

In this low frequency regime we must replace (3.7.33) by

$$J_z \approx I/(\pi a^2)\ . \qquad (3.7.39)$$

Since (3.7.32) is still valid, we find now that

$$J_z \approx I/(\pi a^2)$$

$J_r \approx 2\pi I/(p\lambda) \approx 2\pi I/(2\pi a\lambda) \approx I/(a\lambda)$

so

$$J_r/J_z \approx \pi(a/\lambda) \approx (\pi a)(\omega/2\pi v) \approx \omega a/2v = (\omega a/2)(1/v) \quad . \tag{3.7.40}$$

Using (3.7.38) for $\omega a/2$ we get

$$J_r/J_z < 1/(\mu\sigma a v) \; . \tag{3.7.41}$$

With $\mu = \mu_0 = 4\pi \times 10^{-7}$, $\sigma = 5.81 \times 10^7$ (copper) and $v = c = 3 \times 10^8$ we find for a wire of radius 1 mm,

$$J_r/J_z < \frac{1}{4\pi * 5.81 * 10^{-3} * 3 * 10^8} = \frac{10^{-5}}{4\pi * 5.81 * 3} = 4.6 \times 10^{-8}. \quad \text{low frequency} \tag{3.7.42}$$

The conclusion is that in general $J_r << J_z$ under 10 GHz and finally we justify entries made in the tables of Sections 3.5 and 3.6. The basic fact is that the green cylinder in Fig 3.9 is long, so the surface area through which J_r flows is much larger than the area through which J_z flows.

3.8 Transmission Line Preliminaries

A transmission line normally has two conductors. The cross sectional shape of these conductors is assumed constant in the direction z along the transmission line. The transverse directions are x and y.

A wave propagates down a transmission line in what is called the TEM mode. TEM means that the electric and magnetic fields of a wave traveling down the line are transverse, as in Figures 3.7-9. What this really means is that an electromagnetic wave goes straight down the conductors as guides with no surface reflections, unlike what happens in a waveguide, see Appendix F. Apart from a small drag on the wave due to losses in the conductors, the wave proceeds with wavenumber β_d and velocity v_d as it would in an open medium. The conductors shape the **E** and **B** fields, so the wave is not a "plane wave". Nevertheless, at each point in the dielectric, **E** and **B** are perpendicular (strong skin effect regime) and **E x B** points down the transmission line.

We now summarize a set of basic facts about this TEM mode, most of which were addressed in the previous Section.

Fact 1: The major current for the TEM mode is the *longitudinal* current J_z. We just showed in the last section that $J_r << J_z$. Moreover, $J_\theta = \sigma E_\theta$ vanishes at the surface from (3.7.1) and is presumably either tiny or non-existent inside the conductor. (3.8.1)

Fact 2: There is no cutoff frequency one has to operate above. The TEM mode works all the way down to DC (although at low frequencies, the attenuation per wavelength may become large). See Appendix F for why this is not true in a waveguide. (3.8.2)

Comment: In the low frequency regime of (3.7.3) there is still a TEM wave going down the transmission line, but since we are not then in the strong or extreme skin depth limits, many of the facts of Section 3.7 do not apply. For example, looking at Fig 3.6, the conductors are no longer wrapped by tangent B field lines, and A_z is no longer constant on the conductor perimeter.

Corollary 2: If one operates a transmission line below the cutoff of the lowest waveguide mode, the TEM mode is the only possible way of moving energy down the line. (3.8.3)

Fact 3: The simplest expression of the boundary conditions are in terms of *potentials*, not fields, so the potential wave equations are used to solve problems. For example, a boundary condition might be that the electric potential between the two conductors is 7.5 volts at the driving end. (3.8.4)

Fact 4: The transverse components of the vector potential **A** can be neglected, so A_z is the only component of **A** we have to worry about. (3.8.5)

Proof: This is addressed in Appendix M, but we give a brief summery here. Consider equation (1.5.9) where both conductors have the same μ,

$$\mathbf{A}(\mathbf{x},\omega) = \frac{\mu}{4\pi} \int \mathbf{J}(\mathbf{x}',\omega)\frac{e^{-j\beta R}}{R}\, dV' \qquad (3.8.6)$$

Here, **J** represents the currents in the conductors and the volume integration is over both conductors in x,y and z, and R = |**x**-**x**'|. There is clearly going to be a strong A_z component since the predominant conductor currents are in the longitudinal direction. According to Fact 1 above, transverse currents are very small, so the corresponding transverse components of **A** will also be very small and we shall completely neglect them.

When we compute **A** in the above integral, we can still decompose **A** into A_z, A_r and A_θ . These components are, however, with respect to some fixed coordinate system located perhaps on some approximate center line between the two conductors. Thus, each potential of the pair A_r and A_θ will feel the effect of both J_r and J_θ , but these are both very small. Moreover, there is considerable cancellation which takes place as pieces of J_r and J_θ are added up in the integration. We rely mainly on the fact that J_r and J_θ are very small to conclude that A_r and A_θ may be safely neglected.

This is very different from what happens with A_z. In the region of one conductor, the summation is additive for all nearby pieces of current J_z in that conductor, assuming that the wavelength λ of longitudinal propagation is much larger than any transverse dimension. The only place A_z is small is on a longitudinal line between the conductors where their contributions cancel.

We conclude then that A_r and A_θ can be neglected relative to A_z.

Fact 5: The potential φ(x) can be identified with the transverse "voltmeter voltage" . (3.8.7)

Proof: This is not immediately obvious. The thing one measures as "voltmeter voltage" is the line integral of the electric field between two points. If **E** = - **∇**φ, one can identify φ with this voltmeter voltage, but according to Eq. (1.3.1), we have an extra term to worry about,

$$\mathbf{E} = -\nabla\varphi - \partial\mathbf{A}/\partial t \,. \qquad (3.8.8)$$

However, according to Fact 4 of (3.8.5), the transverse components of **A** are negligible, so

$$\mathbf{E_t} = -\nabla_t \varphi \qquad \text{where} \quad \nabla_t \equiv \hat{\mathbf{x}}\, \partial/\partial x + \hat{\mathbf{y}}\, \partial/\partial y \quad . \tag{3.8.9}$$

If one line-integrates E_t from one conductor to the other (keeping z fixed), one gets $\varphi_1 - \varphi_2$ which is a voltage that a voltmeter would measure.

Fact 6: The potential φ is *constant* over the surface of either conductor at a fixed z. (3.8.10)

This was addressed in (3.7.4) where we had to add the assumptions that we are in the strong or extreme skin effect regimes and we are operating in the transmission line limit. Although φ = constant at ω = 0, we reached no conclusions regarding the general low frequency regime of (3.7.3).

Fact 7: The potential A_z is *constant* over the surface of either conductor at a fixed z. (3.8.11)

This was addressed in (3.7.20) and is only valid in the strong or extreme skin effect regimes. At low frequencies Fact 7 is definitely not valid (see Fig 3.6).

END OF CHAPTER 3 !!!